ELSEVIER

Thermochimica Acta 243 (1994) 209–222

thermochimica acta

The general utility of the *n*th order model in solid state reaction kinetics ☆

J.P. Elder

Merck and Co., Inc., P.O. Box 100, WS-EX, Whitehouse Station, NJ 08889-0100, USA

Received 20 September 1993; accepted 28 January 1994

Abstract

Computerized kinetics analysis of simulated solid state reaction data has been used to demonstrate how the empirical *n*th order model may be employed as a diagnostic tool in thermoanalytical research. The characteristic shape of the curves of the extent and rate of reaction as a function of temperature, generated under non-isothermal conditions, together with the magnitude of the kinetics parameters when this data is subjected to *n*th order Arrhenius analysis, can be utilized to postulate a solid state reaction mechanism, and to calculate the pertinent activation energy and pre-exponential factor. This approach has been employed to analyze the non-isothermal thermogravimetric data characterizing the three stages in the thermal degradation of calcium oxalate monohydrate, postulated to conform to the D4, R3 and D4 mechanisms, respectively. Although the second stage appears to be essentially a single contracting-volume-controlled reaction, the variation of the activation energies and pre-exponential factors with heating rate for the first and third stages implies multiple diffusion-controlled reactions. The procedure has also been used to generate the kinetics parameters of the crystallization of an amorphous form of a candidate drug compound (A2 mechanism) from non-isothermally monitored differential scanning calorimetric data.

Keywords: DSC; DTG; Kinetics; Mechanism; Model; Non-isothermal; Solid state; TG

1. Introduction

All investigators interested in the mechanistic analysis of data pertaining to thermally stimulated reactions in the solid state, are fully aware of the multiplicity

☆ Presented at the 22nd Annual NATAS Conference, Denver, CO, 19–22 September 1993.

SSDI 0040-6031(94)01821-W

of articles in an ever-increasing variety of journals, discussing various aspects of the interpretation of thermoanalytical information, primarily TG and DSC data generated under non-isothermal conditions. The question arises: How does the investigator, using present-day sophisticated instrumentation with its accompanying software, approach this problem? As Málek [1] has stated, it is surprising that reaction kinetics computer programs are so limited with regard to the solid state model algorithms available for analysis of thermal data, generated under non-isothermal conditions. Perrenot and Widmann [2], in discussing the Mettler software package, indicate that the kinetics program allows use of the Šesták–Berggren equation [3]. However, using this empirical equation, the models available are quite limited, and unfortunately are applicable only to isothermally generated data. Faced with this problem in the early eighties, the present author [4] developed Fortran software for the transposition of non-isothermal TG data to dimensionless extent and rate of reaction form, and the reaction kinetics analysis of such information. Algorithms for the nth order and seven solid state models were included. This latter program, TGKIN, was based upon software developed for the investigation of simulated multiple mutually independent reaction systems, program KINMOD [5]. Málek [1] has more recently developed similar all-purpose software. Militký and Šesták [6] have discussed the difficulties encountered in the inverse kinetics problem, i.e. the estimation of the thermodynamic parameters of the correct kinetics model of a reaction from experimental data, generated under non-isothermal conditions. Using data generated for a particular model with defined thermodynamic parameters, they demonstrated an excellent fit using another model with different energetic and entropic parameter values. The nth order is an example of such a model. Thus, despite the observations of Flynn [7] regarding the perhaps too indiscriminate use of the nth order model, when considered purely as an empirical curve-fitting relationship, its use can be of great assistance. The (E,A,n) parameter set, obtained by nth order analysis of non-isothermal data, can be employed, using the rate equation and its integral form, to generate the activation energy and pre-exponential factor for the correct kinetics model. What characteristics of the original data, and the resultant parameter values, can be used to advise the investigator as to the probable correct model? Using simulated non-isothermal TG/DTG data, Dollimore et al. [8] demonstrated their characteristic model features. They pointed out that, with regard to actual experimental TG and DSC data, an inspection of the features can provide a good indication of a probable mechanism. For simulated reactions with the same energetic parameters, the relative positions of extent of reaction data on the temperature axis, and the overall shape of the reaction rate curves together with the relative magnitudes of their maximum values were shown to be characteristic of the kinetics model [9].

Furthermore, although not specifically emphasized at that time, the ratio of E/E_n and $\ln(A/A_n)$ vary markedly with the solid state model, where E,A and E_n,A_n refer to the correct model and nth order parameter values, respectively. Criado et al. [10], emphasizing the fact that, irrespective of the mechanism, non-isothermal data for singular solid state reactions, must, and as shown by Elder [9], does satisfy the nth

order rate equation, listed typical E_n/E ratios. More recently, Koga et al. [11] have developed an equation by which these ratios may be calculated. Málek and Criado [12], in discussing such activation energy ratios, indicate that for any solid state model they vary with the value of E/RT_{max}. Even with a constant E and A, the extent of reaction at the maximum rate can vary with heating rate to a small extent, so one should not be too surprised when nth order analyses yield kinetics parameters which vary with heating rate. It is unfortunate that none of the theoretical papers from the Czech and Spanish schools [1,6,10–12] have presented applications of theory to experimental themoanalytical data. However, Tanaka et al. [13] have presented detailed non-isothermal TG and DSC data characterizing the dehydration of lithium sulfate monohydrate. They have also discussed the so-called distortion of the Arrhenius-derived parameters when an inappropriate solid state model was employed. Peregudov et al. [14] recently presented the results of an nth order Arrhenius analysis of non-isothermal TG and DTA data describing the dehydration of calcium oxalate monohydrate in an inert atmosphere. They indicate a reaction order of 0.5. Dollimore et al. [8] analyzed single heating rate non-isothermal TG data characterizing this reaction in a flowing air environment. On the basis of the shape of the TG/DTG curves, they postulated a three-dimensional diffusion (D4) mechanism.

It is the purpose of this study to show how extent and rate of reaction data for various solid state models may be duplicated exactly by use of nth order-derived kinetics parameters. A relationship for calculating the ratios E/E_n and $\ln(A/A_n)$ that is more general than that given by Koga et al. [11] will be derived. Non-isothermal TG data supportive of postulated mechanisms for the three stages in the ambient pressure, inert atmosphere thermal degradation of calcium oxalate monohydrate will be presented and the reaction kinetics parameters generated. Finally, non-isothermal DSC data characterizing the crystallization of an amorphous pharmaceutical candidate compound in the solid state will be discussed.

2. Simulated solid state reactions

Figs. 1(a) and 1(b) show the complement of the extent of reaction, $1-\alpha$, and reaction rate, $d\alpha/dt$, at a heating rate of 1°C min^{-1} for seven pertinent solid state models [15] all with the same activation energy and pre-exponential factor (E/(kJ mol^{-1}) = 220, $A/min^{-1} = 1.25 \times 10^{15}$) as a function of temperature. These curves were generated as previously described [5] from the general rate equation

$$d\alpha/dt = AT^m e^{-E/RT} f(\alpha) \quad (1a)$$

$$d\alpha/dt = A_n T^m e^{-E_n/RT} f_n(\alpha) \quad (1b)$$

The Arrhenius form of Eq. (1a), namely $m = 0$, was employed. The $\alpha-T$ and $\dot{\alpha}-T$ data were then subjected to nth order Arrhenius analysis according to Eq. (1b). The resultant (E_n,A_n,n) parameter set values are listed in Table 1. Then $(1-\alpha)$ and $d\alpha/dt$ were calculated using these nth order values, and are shown plotted as a

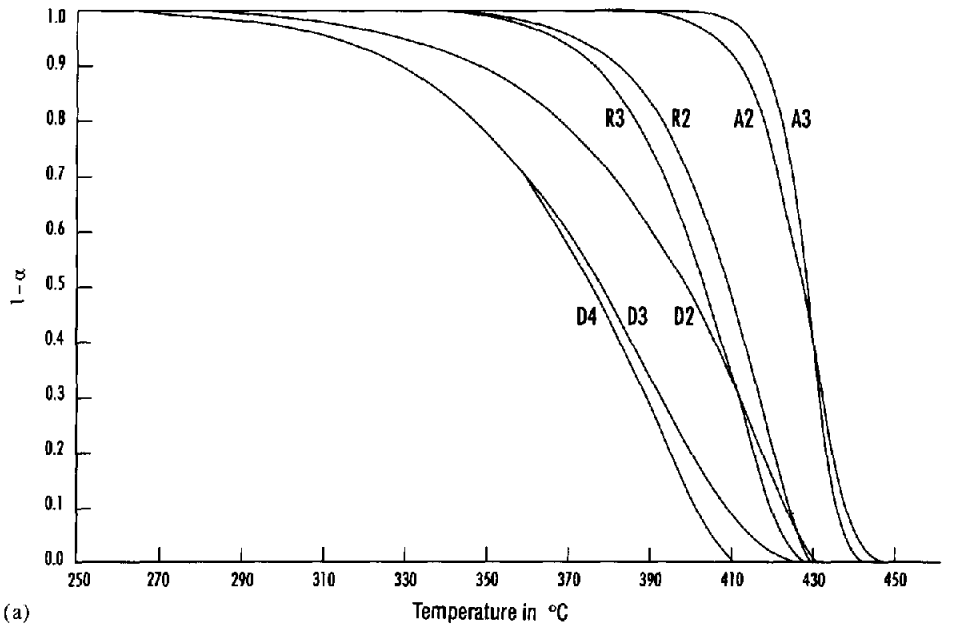

(a)

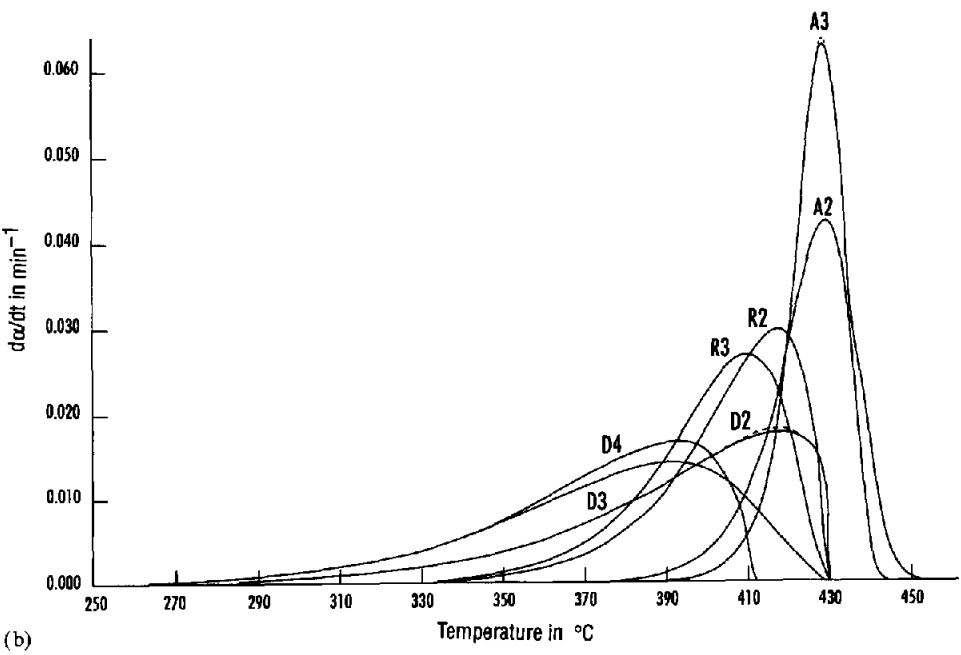

(b)

Fig. 1. (a) Complement of the extent of reaction and (b) reaction rate at 1°C min^{-1} for seven solid state models with $E/(kJ\ mol^{-1}) = 220$ and $A/min^{-1} = 1.25 \times 10^{15}$.

Table 1
Arrhenius kinetics parameters at 1°C min^{-1} [a] for solid state models: $E/(kJ\ mol^{-1}) = 220$, $A/min^{-1} = 1.25 \times 10^{15}$

Model	α_{max}	T_{max} °C	α_{end}	nth order model analyses			Solid state model analyses		
				E_A/ kJ mol^{-1}	A_A/ min^{-1}	n_A	α_{end}	E_A/ kJ mol^{-1}	A_A/ min^{-1}
A2	0.6250	429.7	0.8908	450.2	3.152×10^{32}	0.989	0.9848	220.4	1.336×10^{15}
A3	0.6276	429.8	0.7835	681.1	6.742×10^{49}	0.985	0.9741	220.4	1.356×10^{15}
R2	0.7363	417.3	0.9993	220.1	2.568×10^{15}	0.503	0.9999	220.0	1.250×10^{15}
R3	0.6885	410.3	1.0000	220.1	3.815×10^{15}	0.668	1.0000	220.0	1.252×10^{15}
D2	0.8138	417.8	0.9768	104.6	2.283×10^{6}	0.277	0.9871	219.0	1.039×10^{15}
D3	0.6750	390.8	0.9976	105.6	6.068×10^{6}	0.675	0.9947	220.0	1.269×10^{15}
D4	0.7521	391.8	0.9699	105.2	5.594×10^{6}	0.431	0.9766	219.6	1.161×10^{15}

[a] 0.1°C temperature interval calculations; 1% maximum allowed deviation from linearity in regression.

function of temperature in Figs. 1(a) and 1(b) (broken lines). As can be seen, the two sets of $1-\alpha$ vs. T curves are superimposable. The only differences one can discern are in the $d\alpha/dt$ vs. T curves in the α_{max} region for models A3 and D2. Similar data were obtained at other heating rates in the range 1–100°C min^{-1}. It is easily shown [16] that at the maximum rate of reaction, where $(d^2\alpha/dt^2)_{max}$ is 0, Eqs. (2a) and (2b) apply

$$E/RT_{max}^2 = [-f'(\alpha_{max})/f(\alpha_{max})]\ (d\alpha/dt)_{max}/\beta - m/T_{max} \quad (2a)$$

$$E_n/RT_{max}^2 = [-f'_n(\alpha_{max})/f_n(\alpha_{max})]\ (d\alpha/dt)_{max}/\beta - m/T_{max} \quad (2b)$$

In the special case of $m = 0$, the ratio of Eq. (2a) to Eq. (2b) yields the relationship for E/E_n given by Koga et al. [11]. However, in general, the m/T_{max} term is eliminated by subtraction, yielding the relationship

$$E_n = E - RT_{max}^2/\beta\ (d\alpha/dt)_{max}\ [f'_n(\alpha_{max})/f_n(\alpha_{max}) - f'(\alpha_{max})/f(\alpha_{max})] \quad (3)$$

The values of $f(\alpha)$, $f'(\alpha)$ and their ratios are given in Table 2. Thus

$$E_n = E + RT_{max}^2/\beta\ (d\alpha/dt)_{max}\ C \quad (4)$$

where

$$C = n/(1-\alpha_{max}) + f'(\alpha_{max})/f(\alpha_{max}) \quad (5)$$

From Eqs. (1a) and (1b) one has

$$\ln(A/A_n) = (E - E_n)/RT_{max} + \ln[f_n(\alpha_{max})/f(\alpha_{max})] \quad (6)$$

Using Eqs. (4) and (6), the calculated C, E_n and $\ln(A_n)$ values at 1°C min^{-1} are listed in Table 3a for the seven solid state models indicated and compared (% actual) in the seventh and tenth columns with the Arrhenius-derived values given in Table 1. It should be pointed out that the tabulated E/E_n values are within 99.4%–100.2% of the values calculated using the Koga et al. procedure [11].

Table 2
$f(\alpha)$, $f'(\alpha)$ and $f'(\alpha)/f(\alpha)$ functions for various solid state models

Model	$f(\alpha)$	$f'(\alpha)$ [a]	$f'(\alpha)/f(\alpha)$
Fn	$(1-\alpha)^n$	$-n(1-\alpha)^{n-1}$	$-n/(1-\alpha)$
An [b]	$n(1-\alpha)[-\ln(1-\alpha)]^{1-1/n}$	$(n-1)[-\ln(1-\alpha)]^{(1\ \ n)/n} - n[-\ln(1-\alpha)]^{1-1/n}$	$\dfrac{1-n[1+\ln(1-\alpha)]}{n(1-\alpha)\ln(1-\alpha)}$
Rn [b]	$n(1-\alpha)^{1-1/n}$	$(1-n)(1-\alpha)^{-1/n}$	$(1-n)/[n(1-\alpha)]$
D2	$-[\ln(1-\alpha)]^{-1}$	$-(1-\alpha)^{-1}[-\ln(1-\alpha)]^{-2}$	$[(1-\alpha)\ln(1-\alpha)]^{-1}$
D3	$(3/2)(1-\alpha)^{2/3}/[1-(1-\alpha)^{1/3}]$	$1/2-(1-\alpha)^{-1/3}/[1-(1-\alpha)^{1/3}]^{-2}$	$\dfrac{(1/3)[(1-\alpha)^{1/3}-2]}{(1-\alpha)[1-(1-\alpha)^{1/3}]}$
D4	$(3/2)(1-\alpha)^{1/3}/[1-(1-\alpha)^{1/3}]$	$(-1/2)(1-\alpha)^{-2/3}/[1-(1-\alpha)^{1/3}]^{-2}$	$(-1/3)(1-\alpha)^{-1}[1-(1-\alpha)^{1/3}]^{-1}$

[a] $f'(\alpha) \equiv df(\alpha)/d\alpha$. [b] $n = 2$ and 3.

Table 3a
Calculated nth order parameters for various models at 1°C min^{-1}: $E/(\text{kJ mol}^{-1}) = 220$, $A/\text{min}^{-1} = 1.25 \times 10^{15}$

Model	$[d\alpha/dt]_{max} \times 10^2$ /min^{-1}	$n/(1-\alpha_{max})$	$f'(\alpha_{max})/f(\alpha_{max})$	C	E_n/ kJ mol^{-1}	% Actual	$f_n(\alpha_{max})/f(\alpha_{max})$	ln A_n	% Actual
A2	4.1467	2.6364	−1.3071	1.3293	446.5	99.2	0.5105	74.1867	99.2
A3	6.2208	2.6447	−0.8731	1.7715	672.8	98.8	0.3411	113.3033	98.8
R2	2.9167	1.9083	−1.8962	0.0121	221.4	100.6	0.4979	35.7022	100.6
R3	2.6443	2.1449	−2.1400	0.0049	220.5	100.2	0.3327	35.9513	100.2
D2	1.7368	1.4888	−3.1953	−1.7065	102.4	97.9	1.0550	14.2296	97.2
D3	1.3958	2.0766	−4.3083	−2.2318	105.8	100.2	0.2064	15.6571	100.3
D4	1.6552	1.7368	−3.6167	−1.8799	105.6	100.4	0.2165	15.6008	100.4

Table 3b
Solid state model mean E/E_n and $\ln(A/A_n)$ ratios and $\ln(A/A_n)$ ratio coefficients

Model	Mean values		$\ln(A/A_n) = k_1 + k_2(E/RT_{max})$		
	E/E_n	$\ln(A/A_n)$	k_1	k_2	r^2
A2	0.495 ± 0.009		−4.982	−0.937	−0.9927
A3	0.330 ± 0.008		−8.642	−1.874	−0.9957
R2	0.999 ± 0.013	-0.695 ± 0.909			
R3	0.997 ± 0.010	-1.275 ± 0.665			
D2	2.127 ± 0.040		0.664	0.517	0.9992
D3	2.068 ± 0.040		−0.921	0.503	0.9994
D4	2.081 ± 0.034		−1.013	0.510	0.9992

Analogous calculations have been performed using E and A values varying from 220 to 440 kJ mol^{-1}, and from 1.25×10^{10} to 1.25×10^{35} min^{-1}, respectively, thereby covering the useful temperature range 50–1000°C with an E/RT_{max} range of 25–85. For all the solid state models, the ratio E/E_n remains constant. For the R2 and R3 models, $\ln(A/A_n)$ is also essentially constant. However, for the Avrami and diffusion models, $\ln(A/A_n)$ is a linear function of E/RT_{max}

$$\ln(A/A_n) = k_1 + k_2(E/RT_{max}) \tag{7}$$

Table 3b summarizes the E/E_n, $\ln(A/A_n)$ and Eq. (7) coefficient values. The high r^2 are indicative of an excellent correlation by Eq. (7). Since E/RT_{max} decreases with increase in the heating rate, one finds that for the Avrami (A2, A3) and diffusion (D2, D3, D4) models, $\ln(A/A_n)$ increases and decreases, respectively, with increase in heating rate.

In concluding this discussion of the actual model and effective nth order model Arrhenius analyses, it is pertinent to consider the reversal of the solid state to nth order model transposition. If the $\alpha-T$ and $\dot{\alpha}-T$ data, generated at 1°C min^{-1} using Eq. (1b) with $m = 0$ and the nth order (E_A,A_A,n_A) sets listed in Table 1, are subjected to Arrhenius analyses according to Eq. (1a) with the correct $f(\alpha)$ values, the E_A and A_A parameter values given in the last two columns of Table 1 are obtained; α_{end} indicates the extent of reaction at which the regression analysis was terminated as a result of > 1% deviation from linearity. As seen, α_{end} is close to unity, and the E_A and $\ln(A_A)$ values are within +0.25% and −0.5% of the correct values.

3. Experimental investigations

3.1. Calcium oxalate monohydrate degradation

The ambient pressure, inert atmosphere thermal degradation of calcium oxalate monohydrate was monitored by non-isothermal TG using the Metter TA3500 thermogravimetric system. Loose 200–400 mesh (75–38 μm) ≈10 mg size samples were heated at ten heating rates covering the range 0.25–25°C min^{-1}, in a 100 ml min^{-1}

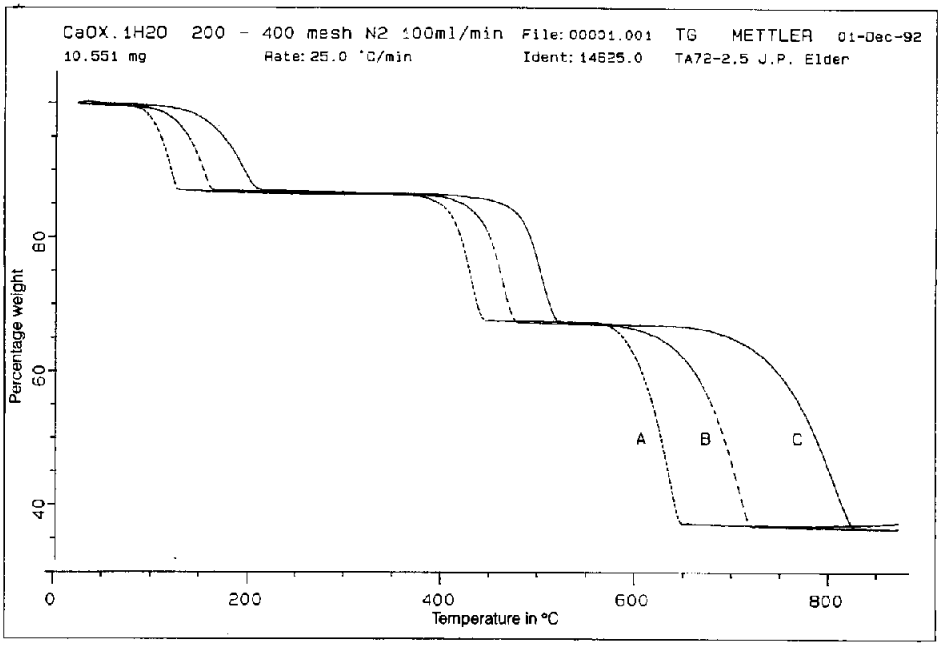

Fig. 2. Experimental TG data (% initial sample weight as a function of temperature) for the thermal degradation of calcium oxalate monohydrate at three heating rates: curve A, 0.25°C min^{-1}; curve B, 2.5°C min^{-1}; and curve C, 25°C min^{-1}.

nitrogen atmosphere from 25 to 850°C. The Mettler special "Calibration 6" [17], using alumel, nickel and trafoperm Curie Point standards, was employed for temperature calibration at each of the several heating rates. Fig. 2 shows the experimental data, percentage of initial sample weight as a function of temperature, at three heating rates: 0.25 (curve A), 2.5 (curve B) and 25°C min^{-1} (curve C). The sectional data at each heating rate for each of the three stages were subjected to nth order Arrhenius analyses using the multilinear regression procedure described by Perrenot and Widmann [2] for the TA72 data analysis and plotting system. The optimum α range for the analyses were selected such that the simulated weight-change curves, based upon the resultant E_n, A_n, n values, overlaid the actual curves as closely as possible over the limits of the reaction step. For steps 1 and 3, for most heating rates, the calculation range was $0.01 < \alpha < 0.99$. For step 2, for $\beta \geq 10$°C min^{-1}, the range was $0.02 < \alpha < 0.92$ and for $\beta < 10$°C min^{-1}, the range was $0.06 < \alpha < 0.99$. Table 4 shows the $(E,\ln(A_n),n)$ values at the several heating rates employed for each step. Fig. 3 shows three sets of percent weight loss data as a function of temperature, both actual and simulated, for each stage: step 1, dehydration at 25°C min^{-1}; step 2, loss of carbon monoxide at 0.5°C min^{-1}; and step 3, loss of carbon dioxide at 5°C min^{-1}. As can be seen from the superimposed curves, the nth order kinetics parameters enable an excellent simulation of the experimental curves. The overall shape of the weight loss curves, together with the constant reaction orders, indicate that the first and third steps are best described by

Table 4
Calcium oxalate monohydrate degradation Arrhenius analysis reaction kinetics parameters

Step	(°C min^{-1})	Experimental nth order data				Arrhenius analysis and calculated solid state parameters				
		T_{max}/°C	E_n/(kJ mol^{-1})	ln(A_n) [a]	n	Model	%D	α_{end}	E/(kJ mol^{-1})	ln(A) [a]
1	0.25	120.3	93.15	24.5043	0.38	D4	5	0.9858	192.72 (193.84)	53.4651 (53.7114)
	0.50	127.7	89.23	23.4145	0.41		2	0.9942	184.61 (185.69)	50.5203 (50.8166)
	1.00	141.8	91.78	23.8942	0.41		2	0.9981	189.90 (190.99)	50.8218 (51.1142)
	2.50	153.4	77.28	19.7643	0.42		3	0.9947	160.95 (160.82)	41.8325 (41.8779)
	5.00	169.1	77.02	19.5443	0.42		2	0.9926	160.48 (160.28)	40.7111 (40.7620)
	7.50	174.7	71.52	18.1243	0.43		3	0.9837	149.15 (148.83)	37.4270 (37.4958)
	10.00	182.2	71.13	17.9544	0.43		5	0.9880	148.47 (148.02)	36.8347 (36.8811)
	15.00	191.0	68.48	17.2543	0.42		3	0.9908	143.26 (142.51)	35.0973 (35.0747)
	20.00	194.4	66.05	16.7446	0.42		3	0.9904	138.32 (137.45)	33.7970 (33.7642)
	25.00	195.3	62.96	16.0943	0.43		5	0.9818	131.84 (131.02)	32.2177 (32.2373)
2	0.25	432.4	291.55	45.6744	0.64	R3	2	0.9844	292.70 (290.68)	44.7962 (44.3994)
	0.50	442.4	289.41	45.2743	0.66		1	0.9983	289.80 (288.54)	44.2487 (43.9993)
	1.00	452.0	285.47	44.6345	0.67		1	0.9999	285.26 (284.61)	43.4968 (43.3595)
	2.50	464.6	286.89	44.9443	0.67		1	0.9991	286.70 (286.03)	43.8112 (43.6693)
	5.00	479.5	291.35	45.3943	0.68		3	0.9850	290.78 (290.48)	44.1921 (44.1193)
	7.50	486.8	294.43	45.8343	0.68		5	0.9915	293.77 (293.55)	44.6178 (44.5593)
	10.00	490.4	302.88	47.2544	0.66		5	0.9969	303.28 (301.97)	46.2256 (45.9794)
	15.00	498.7	308.99	48.0943	0.66		5	0.9768	309.27 (308.06)	47.0451 (46.8193)
	20.00	504.7	308.86	47.9743	0.66		10	0.9658	309.14 (307.93)	46.9253 (46.6993)
	25.00	507.5	308.84	48.0143	0.66		10	0.9186	309.07 (307.91)	46.9550 (46.7393)
3	0.25	634.5	284.67	33.1844	0.43	D4	2	0.9928	582.78 (592.40)	71.1590 (72.2063)
	0.50	655.6	267.07	30.6342	0.41		2	0.9967	548.80 (555.77)	65.6119 (66.3273)
	1.00	677.0	247.68	27.9746	0.41		2	0.9988	510.31 (515.42)	59.9078 (60.2361)
	2.50	704.3	223.97	24.9444	0.41		2	0.9983	463.00 (466.08)	52.8428 (53.1802)
	5.00	735.8	222.01	24.4744	0.42		2	0.9942	458.84 (462.00)	51.1804 (51.5490)
	7.50	750.9	221.64	24.4144	0.42		2	0.9934	458.30 (461.23)	50.6925 (51.0287)
	10.00	762.3	211.68	23.1846	0.41		3	0.9987	438.90 (440.51)	48.0527 (48.2673)
	15.00	780.6	207.42	22.6144	0.43		3	0.9876	429.86 (431.64)	46.4489 (46.7276)
	20.00	794.9	202.45	21.9743	0.43		5	0.9912	420.14 (421.30)	44.9348 (45.1572)
	25.00	802.9	200.92	21.8345	0.42		3	0.9938	417.60 (418.11)	44.5122 (44.6557)

[a] A in min^{-1}.

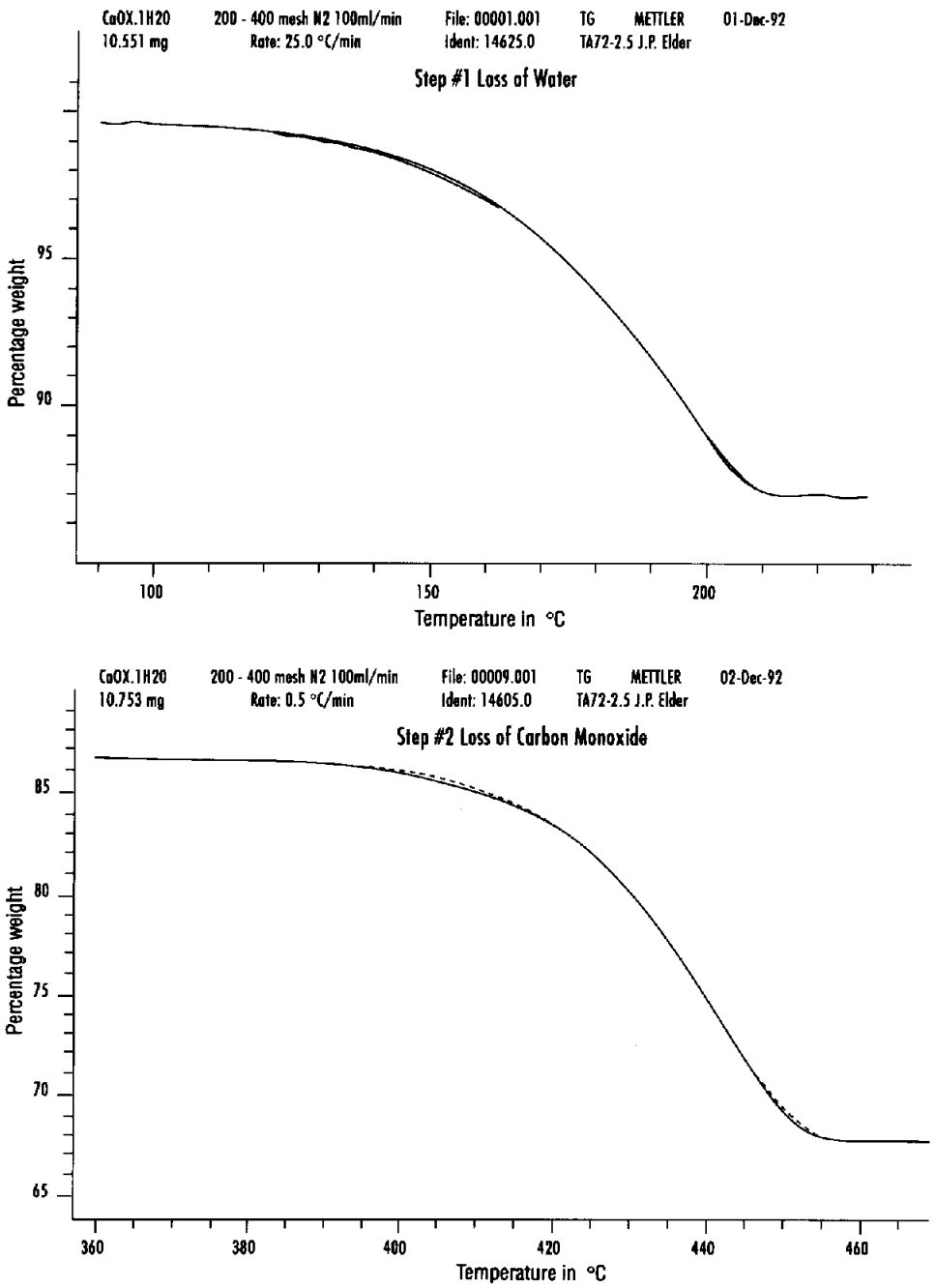

Fig. 3. Experimental and simulated TG data for the three steps in the thermal degradation of calcium oxalate monohydrate: step 1 at 25°C min^{-1}, step 2 at 0.5°C min^{-1} and step 3 at 5°C min^{-1}. Continued on next page.

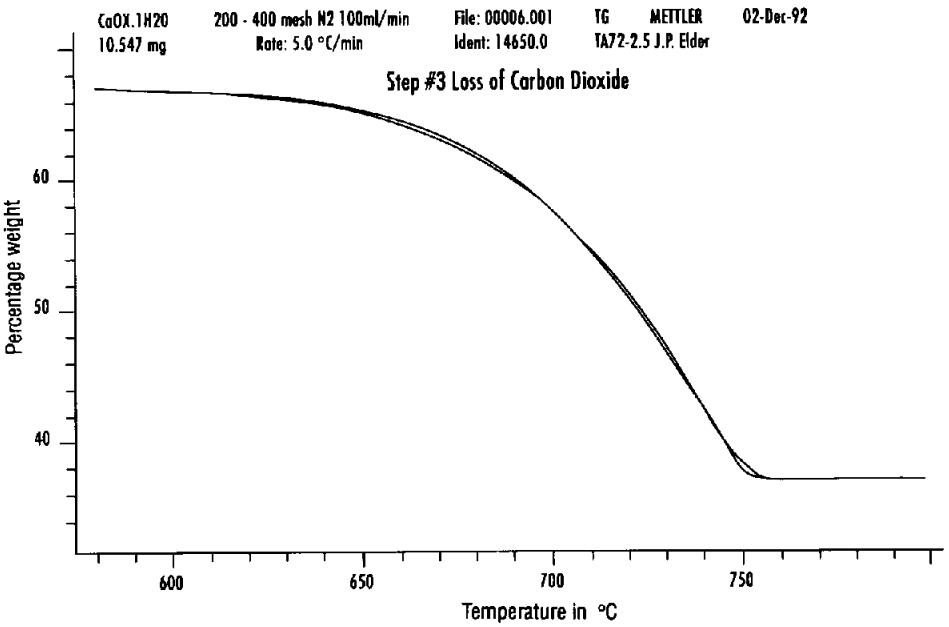

the D4 three-dimensional diffusion model mechanism, while the second step appears to follow the R3 contracting volume model mechanism. Using program KINMOD [5] with the tabulated $(E_n,\ln(A_n),n)$ sets at each heating rate, extent and rate of reaction data were generated as a function of temperature, and then an Arrhenius analysis performed using the D4, R3 and D4 $f(\alpha)$ models, respectively. The correct E and $\ln(A)$ kinetics parameters are listed in Table 4. The allowed percentage deviations ($\%D$) from linearity in these regressions were chosen such that the analyses were terminated at $\alpha_{end} \geq 0.98$ in most cases, step 2 R3 analyses at $>15°C\ min^{-1}$ being the exceptions.

Using the E/E_n ratios in Table 3b, the correct activation energies, E, and the appropriate E/RT_{max} values may be calculated. The pertinent $\ln(A/A_n)$ value is then selected (model R3) or calculated (model D4) using the Eq. (7) coefficients. Then $\ln(A)$ is easily obtained. Values thus calculated are given in parentheses in Table 4. As can be seen, the calculated parameter values are within $\pm 0.7\%$ of the Arrhenius analysis values, attesting to the correctness of the "ratio calculation" procedure.

For the dehydration step in an air atmosphere at $20°C\ min^{-1}$, Dollimore et al. [8] proposed a D4 mechanism with $E/(kJ\ mol^{-1}) = 143.3$ and $A/min^{-1} = 5.59 \times 10^{13}$, values that compare favorably with those given in Table 4 at this heating rate.

3.2. *Crystallization of an amorphous pharmaceutical compound*

In assessing the possibility of an undesirable crystallization of an amorphous drug candidate during a spray-drying operation, DSC was employed to study the

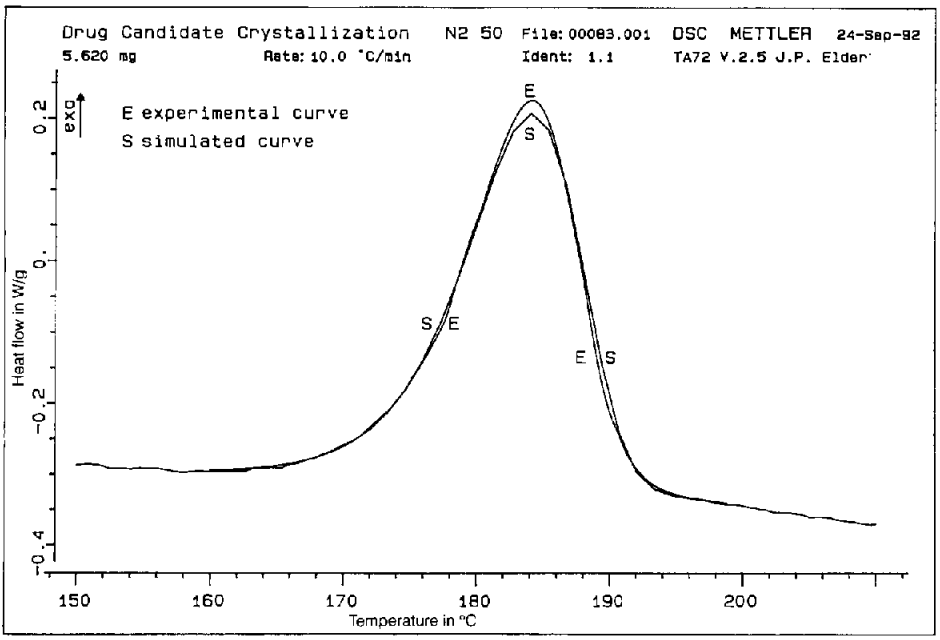

Fig. 4. Experimental DSC data (normalized heat flow as a function of temperature) at 10°C min^{-1} for the crystallization of a pharmaceutical compound from the amorphous state.

thermal behavior of the compound. The Mettler TA 3300 differential scanning calorimetric system was employed for this measurement. Open aluminum crucibles in a 50 ml min^{-1} flowing dry nitrogen atmosphere were used. Fig. 4 shows the weight-normalized exothermic heat flow characterizing the crystallization at 10°C min^{-1}. The maximum rate occurred at 62.1% extent of reaction at 184.2°C; nth order Arrhenius analysis was performed on the data between 176 and 188°C (10–90% extent of reaction), yielding $E_n/(\text{kJ mol}^{-1}) = 424.4 \pm 1.1$, $\ln(A_n/\text{min}^{-1}) = 112.54 \pm 0.3$ and $n = 1.08 \pm 0.02$. These values are consistent with the two-dimensional random nucleation mechanism, model A2 [9,18]. Accordingly, these nth order parameters were used as input for program KINMOD [5] and an A2 model Arrhenius analysis carried out, yielding $E/(\text{kJ mol}) = 208.1$ and $\ln(A/\text{min}^{-1}) = 54.955$. Using the "ratio procedure" one obtains $E/(\text{kJ mol}^{-1}) = 210.1$ and $\ln(A/\text{min}^{-1}) = 55.792$, values $\approx 1\%$ above the Arrhenius analysis parameters, again attesting to the accuracy of this procedure.

4. Conclusions

The use of the nth order empirical model in the rate equation is a highly useful tool in characterizing thermally stimulated solid state reactions monitored under non-isothermal conditions by DSC and/or TG. The value of the reaction order

resulting from Arrhenius analysis of such data, together with the characteristic shapes of the $\alpha-T$ (TG) and/or $\dot{\alpha}-T$ (DSC, DTG) curves, enables a realistic assessment of the reaction mechanistic model. It appears not to matter how the $(E_n,\ln(A_n),n)$ parameter set is obtained, using the thermoanalytical instrument supporting software (Borchardt–Daniels, Multilinear Regression or the Freeman–Carroll method), provided it can be shown that the derived kinetics parameters enable an excellent data curve fit.

The characteristic values of the activation energy ratios E/E_n and the logarithmic ratios of the pre-exponential factors $\ln(A/A_n)$ enable an evaluation of the chosen model kinetics parameters, which are within $\pm 1\%$ of the values resulting from a complete Arrhenius analysis.

For single reactions, the nth order or correct model kinetics parameters vary very little with heating rate and, as previously discussed [9], yield essentially constant activation energies when subjected to peak (Kissinger [19]) or isoconversional (Friedman [20]) analysis. There are minor variations in the pre-exponential factor values, the magnitudes of which are dependent upon the actual solid state model. To a large degree, this appears to be exemplified by the second stage in the thermal degradation of calcium oxalate monohydrate. However, for the first and third diffusion-controlled stages in this step-wise decomposition, one observes significant changes in the nth order and, therefore, in the chosen model kinetics parameters. For single reactions, isoconversionally generated kinetics parameters can be employed to calculate, at any heating rate, $\alpha-T$ data compatible with those resulting from the single heating rate Arrhenius analysis, provided one makes allowance for the correct model in the pre-exponential factor values. However, this is not the case if the experimental or computer-simulated data are, in fact, the effective result of a set of multiple reactions operating in a mutually independent fashion. This aspect of thermally stimulated solid state kinetics will be discussed in more detail in a future publication.

References

[1] J. Málek, Thermochim. Acta, 200 (1992) 257.
[2] B. Perrenot and G. Widmann, J. Therm. Anal., 37 (1991) 1785.
[3] J. Šesták and G. Berggren, Thermochim. Acta, 3 (1971) 1.
[4] J.P. Elder, Thermochim. Acta, 95 (1985) 33; 95 (1985) 41.
[5] J.P. Elder, J. Therm. Anal., 29 (1984) 1327; 34 (1988) 1467.
[6] J Militký and J. Šesták, Thermochim. Acta, 203 (1992) 31.
[7] J.H. Flynn, Thermochim. Acta, 203 (1992) 519.
[8] D. Dollimore, T.A. Evans, Y.F. Lee, G.P. Pee and F.W. Wilburn, Thermochim. Acta, 196 (1992) 255.
[9] J.P. Elder, J. Therm. Anal., 30 (1985) 657.
[10] J.M. Criado, M. Gonzalez, A. Ortega and C. Real, J. Therm. Anal., 34 (1988) 1387.
[11] N. Koga, J. Šesták and J. Málek, Thermochim. Acta, 188 (1991) 333.
[12] J. Málek and J.M. Criado, Thermochim. Acta, 203 (1992) 25.
[13] H. Tanaka, N. Koga and J. Šesták, Thermochim. Acta, 203 (1992) 203.
[14] A.N. Peregudov, T.V. Peregudova and L. Karpov, Thermochim. Acta, 197 (1992) 21.

[15] M.E. Brown, D. Dollimore and A.K. Galwey, in C.H. Bamford and C.F.H. Tipper (Eds.), Comprehensive Chemical Kinetics, Vol. 22, Elsevier, New York, 1980, Chapter 3, p. 90.
[16] J.P. Elder, in P.S. Gill and J.F. Johnson (Eds.), Analytical Calorimetry, Vol. 5, Plenum Press, New York, 1984, p. 255.
[17] Mettler TA 3000 System Operational Instructions, Appendix G, p. 324. Mettler-Toledo AG, Sonnenberg Strasse 74, Schwezenbach, CH-8603, Switzerland.
[18] J.P. Elder, J. Therm. Anal., 36 (1990) 1077.
[19] H.E. Kissinger, J. Res. Natl. Bur. Stand., 57 (1956) 217.
[20] H.L. Friedman, J. Polym. Sci., 6C (1965) 183.